Inorganic Chemistry

Article

pubs.acs.org/IC

Copper(I) Complexes of Pyridine-Bridged Phosphaalkene-Oxazoline Pincer Ligands

Spencer C. Serin, Fraser S. Pick, Gregory R. Dake,* and Derek P. Gates*

Department of Chemistry, University of British Columbia, 2036 Main Mall, Vancouver, British Columbia, Canada

Supporting Information

ABSTRACT: The synthesis of enantiomerically pure pyridine-bridged phosphaalkene-oxazolines ArP═C(Ph)(2,6-C_5H_3NOx) (**1**, Ar = Mes/Mes*, Ox = CNOCH(*i*-Pr)-CH_2/CNOCH(CH_2Ph)CH_2) is reported. This new ligand forms a κ(P), κ^2(NN) dimeric complex with copper(I) (**7**) that dissociates into a cationic κ^3(PNN) monomeric complex upon addition of a neutral ligand {[**1a**·CuL]OTf (**8a**–**e**): L = PPh_3 (**a**), $P(OPh)_3$ (**b**), 2,6-lutidine (**c**), 4-DMAP (**d**), 1-methylimidazole (**e**)}. The P–Cu bond lengths in **8** are influenced by the π-accepting/σ-donating properties of L, and this can be observed by changes in the $\delta^{31}P_{P=C}$ NMR shift. The donor–acceptor properties in complexes of type **8** have also been investigated by UV/vis spectroscopy and density functional theory calculations.

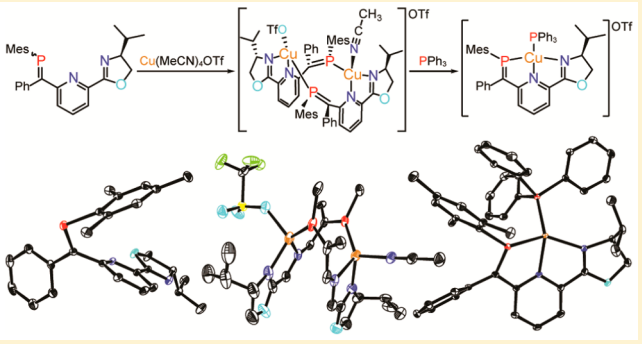

INTRODUCTION

The tridentate pincer motif, a classic framework, is often used to investigate both profound and subtle steric and electronic effects within ligand design.[1] 2,6-Disubstituted pyridines are well recognized as obvious chemical systems for the creation of tridentate pincer ligand sets. Often these pyridines are difunctionalized with common donor sets based on N, O, S, and P atoms. Although symmetric ligands can be easier to synthesize, nonsymmetric 2,6-substituted pyridines offer the possibility of fortuitous binding properties by forced orientation of different donors in a *trans*-geometry within a metal complex (e.g., **A** and **B** in Figure 1).[2]

There is considerable interest in the coordination chemistry of compounds containing low coordinate phosphorus, such as phosphaalkenes or phosphinines, for potential applications in catalysis.[3,4] The P═C double bond features a low-energy π^*-orbital that leads to excellent π-accepting properties.[5] The most studied[6] phosphaalkene-containing pincer ligand motif is the symmetric ligand **D** [i.e., 2,6-bis(phosphaethylene)pyridine or BPEP, R = H[7] and R = Ph[8]]. This class of ligand has attracted attention due to its highly delocalized π-electron backbone that is not found in analogous bisphosphine derivatives. BPEP-Ph offers distinctive metal stabilization properties that permit the isolation of a four-coordinate Fe(I) species [e.g., (BPEP-Ph)FeBr] in an unusual 15-electron configuration.[8,9] Additionally, BPEP-Cu(I) complexes {e.g., Cu(X)(BPEP-Ph), where X = $[PF_6]^-$ and $[SbF_6]^-$} are extremely electron-deficient, exhibiting strong affinity toward both $[PF_6]^-$ and $[SbF_6]^-$, as a consequence of the strong π-accepting ability of the P═C bonds.[10,11]

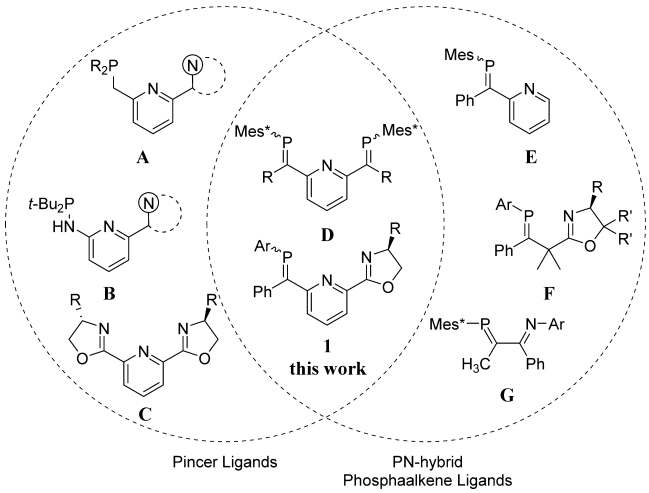

Figure 1. Selected examples of pincer and mixed PN phosphaalkene ligands.

We have previously developed *bidentate* ligands such as the achiral phosphaalkene-pyridine **E**[12] which is an effective ligand for the Pd(II)-catalyzed Overman–Claisen rearrangement of allyl trichloroacetimidates.[13] In addition, we have developed a modular route to the first enantiomerically pure phosphaalkene-oxazoline ligands (**F**, PhAk-Ox)[14,15] and have demonstrated their utility in the Pd(II)-catalyzed asymmetric allylic alkylation reaction.[16] Related work involves the use of the

Received: April 13, 2016

DOI: 10.1021/acs.inorgchem.6b00917
Inorg. Chem. XXXX, XXX, XXX–XXX

mixed phosphaalkene-imine ligand **G** for the Pd(II)-catalyzed oligomerization of ethylene.[17] Inspired by the ubiquity of bisoxazoline pyridine pincer ligands (**C**, PyBox) in asymmetric catalysis,[18] we envisioned the development of a hybrid phosphaalkene-pyridine-oxazoline PNN ligand (**1**).

In this report, we present the modular synthesis of enantiomerically pure phosphaalkenes **1a–c** (PhAk-Pyr-Ox) as a new ligand class that effectively coordinates to Cu(I). This hybrid PNN ligand increases the sophistication possible for low-coordinate phosphorus compounds as well as provides a new nonsymmetric PNN-pincer motif for application in coordination chemistry.

RESULTS AND DISCUSSION

Phosphaalkene Synthesis and Characterization. The general synthetic strategy toward phosphaalkene **1** is outlined in Scheme 1. By analogy to PhAk-Ox and PyBox, the strategy

Scheme 1. Synthetic Approach to Pyridine-Bridged Phosphaalkene-Oxazolines

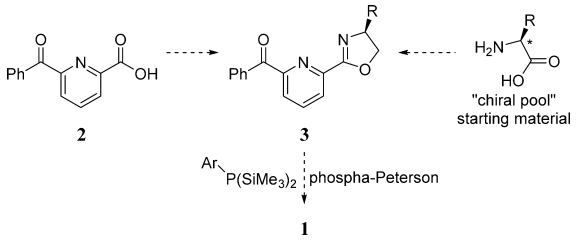

takes advantage of well-established literature condensation reactions. Specifically, the condensation of α-silylphosphides with ketones, the *phospha*-Peterson reaction, generates phosphaalkenes in high yield.[12] Similarly, the (multistep) condensation of chiral pool derived α-amino alcohols with carboxylic acids produces oxazolines. Consequently, ketones of type **2** are critical synthetic building blocks. Ketones of type **2** could be conveniently prepared from a mono esterified derivative of 2,6-pyridine dicarboxylic acid.

Carboxylic acid **4** can be prepared from commercially available 2,6-pyridinedicarboxylic acid.[19] Reaction of **4** with thionyl chloride generates an acid chloride that undergoes Friedel–Crafts acylation with benzene in the presence of $AlCl_3$ (Scheme 2). The acidic workup of this acylation also hydrolyzed the methyl ester to afford 6-benzoyl-2-pyridine-carboxylic acid (**2**) as an off-white solid in a 68% overall yield. Importantly, only solvent extraction was required to purify large batches (ca. 20 g) of acid **2**. Analysis of the $^{13}C\{^1H\}$ NMR spectrum of **2** revealed the expected characteristic signals for the C═O carbon of the benzoyl and carboxylic acid ($\delta^{13}C$ = 192.1 and 163.7) respectively.

A multistep procedure to oxazolines **3a–b** from **2** was adopted from a previous report.[20] Amides **5a-b** could be prepared in a straightforward manner by the reaction of the acid chloride derived from **2** and either L-valinol (**a**) or L-phenylalaninol (**b**), (Scheme 2). The alcohol functions in **5a-b** could be converted to chlorides **6a-b** using $SOCl_2$ in hot $CHCl_3$. A traditional cyclization[21] of related chlorides to form oxazolines that used alkaline aqueous conditions (NaOH in refluxing $MeOH/H_2O$) was not possible in this instance due to the hydrolytic instability of the oxazoline product. Fortunately, cyclization was successful under anhydrous conditions using NaH in refluxing THF, as no aqueous workup step was required to afford ketones **3a-b**. Importantly, these steps can be performed without thorough purification of the amides **5a-b** and chlorides **6a-b**.

Recrystallization of the oxazolines **3a-b** in Et_2O afforded analytically pure ketones in 45% and 66% yield, respectively. Compounds **3a-b** were fully characterized using ^1H and $^{13}C\{^1H\}$ NMR spectroscopy and mass spectrometry. Particularly diagnostic are the $^{13}C\{^1H\}$ NMR signals for the C═N of the oxazoline and C═O of the ketone in **3** {$\delta^{13}C$ [C═N, C═O] = (**3a**): 161.9, 192.1; (**3b**): 162.6, 192.2}. Each ketone displayed optical activity {$[\alpha]_D^{22}$ = **3a**: −118° $cm^3\ g^{-1}\ dm^{-1}$ (c = 2.2×10^{-1}, $CHCl_3$); **3b**: −47.6° $cm^3\ g^{-1}\ dm^{-1}$ (c = 2.8×10^{-1}, $CHCl_3$)}. Crystals of ketone **3a** were obtained by slow evaporation of a saturated Et_2O solution. The resulting solid state molecular structure [Figure 2a], confirmed the configuration of the (*S*)-stereocenter of the amino alcohol in the oxazoline.

The *phospha*-Peterson reaction[12] was performed as the P═C bond forming step (Scheme 2). The representative procedure is as follows: a solution of ketone **3a** in THF was added dropwise to a cooled (−78 °C) solution of $MesP(Li)SiMe_3$ in THF. The reaction was warmed to room temperature whereupon an aliquot was removed for analysis by ^{31}P NMR spectroscopy. The signal assigned to $MesP(Li)SiMe_3$ (δ = −187) was replaced by two new signals of equal intensity at 266.6 and 248.3 ppm, in a range consistent with those expected for phosphaalkenes[12] and indicating the product was formed as a

Scheme 2. Synthesis of Pyridine-Bridged Phosphaalkene-Oxazolines

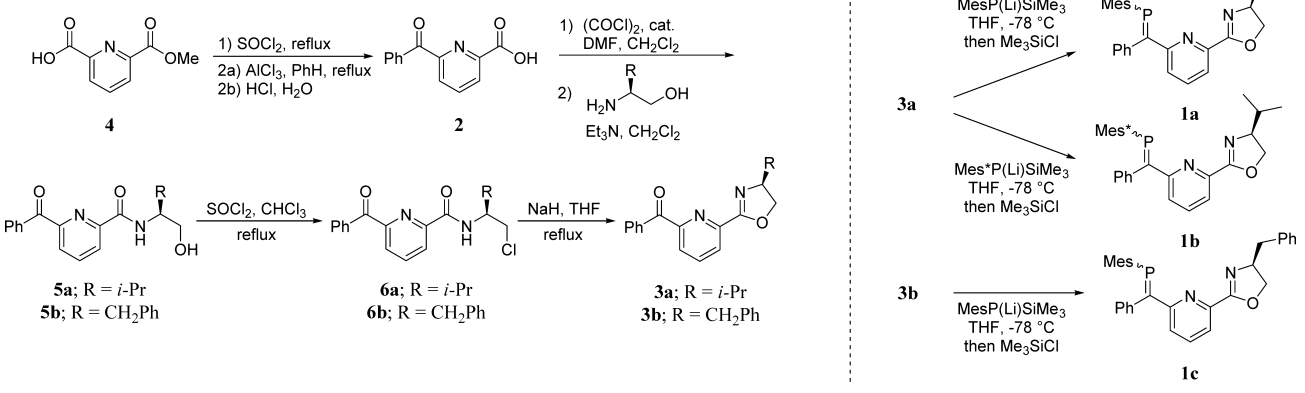

DOI: 10.1021/acs.inorgchem.6b00917
Inorg. Chem. XXXX, XXX, XXX–XXX

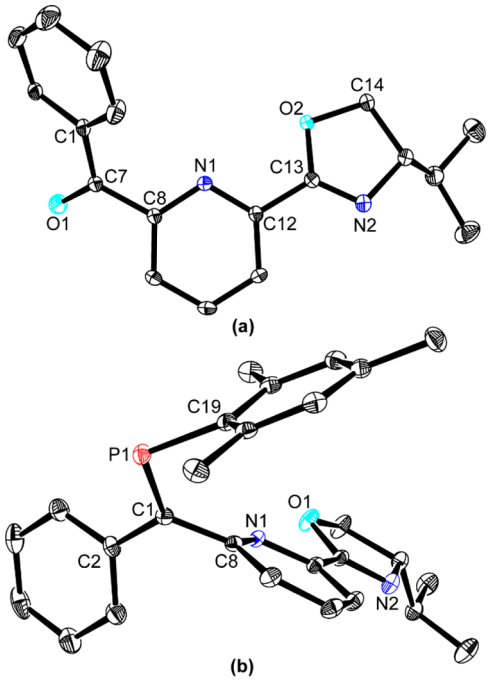

Figure 2. Molecular structures of (a) **3a** and (b) *Z*-**1a**. Thermal ellipsoids are drawn at the 50% probability level. Hydrogen atoms omitted for clarity. Selected bond lengths (Å) and angles (deg): **3a**: O(1)−C(7) 1.217(2), N(2)−C(13) 1.268(2), O(2)−C(13) 1.353(2), C(1)−C(7)−C(8) 120.9(2), C(12)−C(13)−O(2) 117.0(1), C(12)−C(13)−N(2) 123.5(2), O(2)−C(13)−N(2) 119.4(2). *Z*-**1a**: P(1)−C(1) 1.693(2), P(1)−C(19) 1.834(2), C(1)−C(2) 1.488(3), C(1)−C(8) 1.491(3), C(1)−P(1)−C(19) 104.2(1), C(2)−C(1)−P(1) 119.3(2), C(8)−C(1)−P(1) 125.4(2), and C(2)−C(1)−C(8) 115.2(2).

mixture of *E* and *Z* stereoisomers. The desired phosphaalkene **1a** (yield = 54%) was isolated by trituration with hexanes to give the product as a red solid (ca. 1.0:0.64, *Z*:*E*) and crystallographically characterized as the *Z*-isomer after recrystallization from benzene [Figure 2b]. Overall the metrical parameters are consistent with those observed previously for Mes-substituted phosphaalkenes such as MesP═CPh$_2$ and related systems.[12,22]

Phosphaalkene **1a** was fully characterized using ^{1}H, ^{13}C{^{1}H}, and ^{31}P{^{1}H} NMR spectroscopy, and mass spectrometry [HRMS (**1a**$^+$): *m*/*z* 428.2018 (found); 428.2016 (calcd)]. Signals could be unequivocally assigned to either the *Z*- or *E*-isomer by using ^{1}H−^{1}H NOESY, ^{1}H−^{1}H COSY, and ^{31}P-{^{1}H}-^{1}H HSQC NMR spectroscopy (Figures S1 and S2, Supporting Information). Consistent with previous reports of pyridyl-substituted phosphaalkenes, the more upfield ^{31}P{^{1}H} NMR signal is indicative of a *Z*-isomer [e.g., δ^{31}P = MesP═CPh(2-py): 260.1 (*E*), 242.1 (*Z*);[12] Mes*P═CH(2-py): 285.4 (*E*), 259.6 (*Z*)[7]].

To illustrate the modularity of our synthetic route to chiral phosphaalkenes, two additional phosphaalkenes **1b** and **1c** were prepared in 27% and 42% yields, respectively. These compounds were prepared following the same procedure as described for **1a**. The steric bulk of the *P*-substituent is increased in **1b** by employing the Mes* moiety. Additionally, by using ketone **3b** instead of **3a**, a benzyl moiety (**1c**) was substituted in place of the isopropyl group (**1a**). Each new phosphaalkene was characterized by ^{31}P{^{1}H} NMR spectroscopy [δ^{31}P = **1b**: 266.0 (*E*), 257.6 (*Z*); **1c**: 264.4 (*E*), 245.5 (*Z*)], ^{1}H/^{13}C NMR spectroscopy, spectroscopy and mass spectrometry [HRMS (**1b**$^+$): *m*/*z* 555.3491 (found); 555.3504 (calcd), (**1c**$^+$): *m*/*z* 476.2018; 476.2018 (calcd)].

Coordination of 1a to Copper. The coordination chemistry of PNN-proligand **1a** is of considerable interest. As a starting point, we investigated binding of **1a** to copper(I) since related NNN-pincer complexes have been used in a variety of asymmetric transformations, such as hydrosilylations,[23,24] aziridinations,[25] alkyne additions to imines,[26] and conjugate additions,[27,28] among others. Moreover, copper(I) complexes of phosphaalkene-pyridine ligands have been reported previously.[7,10,11,29,30]

A mixture of **1a** and Cu(MeCN)$_4$OTf in CH_2Cl_2 was stirred for 2 h over which time a color change from red to deep brown was observed (Scheme 3). Analysis of an aliquot using ^{31}P{^{1}H} NMR spectroscopy revealed quantitative conversion of the signals for both isomers of phosphaalkene **1a** to a single new resonance at 186 ppm, a value shifted considerably upfield relative to pincer precursor *E*-**1a** ($\Delta\delta$ = −62). The appearance of a single resonance in the ^{31}P{^{1}H} NMR spectrum of the reaction mixture suggests isomerization of the ligand prior to coordination. An upfield shift of >60 ppm for **1a** and Cu(I) is larger than any previously reported copper(I) phosphaalkene-pyridine complexes [$\Delta\delta$ = {*E*-Mes*P═C(2-Py)(H)}Cu-(MeCN)$_2^+$: −15 ppm;[7] (BPEP-Ph)Cu(SbF$_6$): −35 ppm;[10] (BPEP-H)Cu(MeCN)$^+$: −16 ppm[30]]. The product was precipitated by addition of Et$_2$O, and filtered to give complex **7** as a brown solid in 79% yield.

Scheme 3. Synthesis of Copper(I)-phosphaalkene Complexes

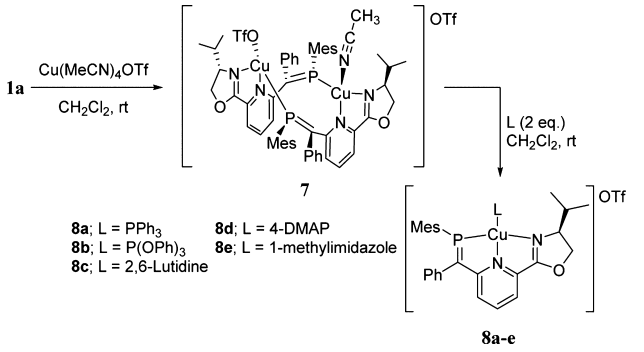

Single crystals of complex **7** were obtained by slow diffusion of Et$_2$O into a CH_2Cl_2 solution. X-ray crystallographic analysis produced the structure of an unexpected dimeric Cu(I) complex [Figure 4a]. Phosphaalkene **1a** did not coordinate to copper as a neutral κ^3(PNN) ligand as expected, but rather κ(P), κ^2(NN). Each Cu(I) is bound to an oxazoline-pyridine moiety in addition to the phosphaalkene of a neighboring **1a** molecule. This coordination mode has not been observed for related BPEP-Cu(I) complexes. The closest example is the dimeric copper complex **H** (Figure 3) which was isolated from the reaction of (*S*,*S*)-*i*-Pr-PyBox with Cu(MeCN)$_4$PF$_6$. Unlike complex **7**, the Cu(I) centers in **H** have different coordination numbers. In each case, the pincer serves as a bridging ligand.

It should be noted that the steric environment around the Mes-substituted phosphorus atom in **1a** is smaller than that of the Mes*-substituted phosphorus atoms within BPEP. Therefore, ligand **1a** is more likely to form a bridging dimeric complex such as **7**, while all the previously reported BPEP

DOI: 10.1021/acs.inorgchem.6b00917
Inorg. Chem. XXXX, XXX, XXX−XXX

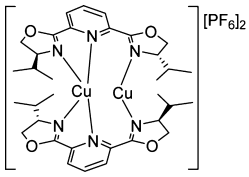

H

Figure 3. Known dimeric copper pyridine-oxazoline complex.

complexes are monomeric. It was envisioned that substituting the weakly coordinating $^{-}$OTf and MeCN ligands in **7** with a larger neutral ligand (L, Scheme 3) would facilitate the isolation of a monomeric $[(PNN)Cu(L)]^{+}$ complex. Fittingly, upon addition of a bulky ligand (2 equiv) to complex **7** (1 equiv) the reaction color drastically changed from deep brown to dark red [L = PPh_3 (**8a**) and $P(OPh)_3$ (**8b**)], dark green [L = 2,6-lutidine (**8c**)], or dark blue [L = 4-DMAP (**8d**) and 1-methylimidazole (**8e**)]. In each case, analysis of the $^{31}P\{^{1}H\}$ NMR spectra of the reaction mixture showed complete conversion of complex **7** to a new product with a distinct chemical shift (**8a**: 232 ppm; **8b**: 227 ppm; **8c**: 215 ppm; **8d**: 208 ppm; **8e**: 207 ppm). Additionally, for **8a** and **8b**, the free phosphine and phosphite signals ($\delta^{31}P$ = −6 and 129, respectively) were replaced by new resonances ($\delta^{31}P$ = 9 and 114, respectively), which were tentatively assigned to coordinated phosphine or phosphite.

Complex **8a** was isolated and crystals suitable for X-ray diffraction were obtained by the diffusion of hexanes into a THF solution. Analysis of the solid state molecular structure revealed the monomeric $[(PNN)Cu(PPh_3)]^{+}$ complex [Figure 4b].

Characterization of Copper Complexes. In addition to obtaining the solid state molecular structures for complexes **7** and **8a**, both complexes were characterized by ^{1}H, $^{13}C\{^{1}H\}$, $^{19}F\{^{1}H\}$, and $^{31}P\{^{1}H\}$ NMR analysis, elemental analysis (for **7**) and mass spectroscopy (for **8a**). Complexes **7** and **8a** showed an optical rotation $\{[\alpha]_D^{22}$ = **7**: −24.7° cm^3 g^{-1} dm^{-1} (c = 1.8 × 10^{-1}, CH_2Cl_2); **8a**: 89.2° cm^3 g^{-1} dm^{-1} (c = 0.72 × 10^{-1}, CH_2Cl_2)$\}$. Complex **7** displayed remarkable air and moisture stability as a solid and could be stored for weeks on the benchtop with no signs of degradation (by $^{31}P\{^{1}H\}$ NMR analysis), while **8a** decomposed in ambient conditions. The NOESY NMR spectrum of complex **7** in $CDCl_3$ (Figure S3, Supporting Information) suggests the dimer remains stable in solution and does not dissociate into two monomeric copper complexes. In particular, a NOE correlation was observed between one ortho-CH_3 group of the *P*-Mes substituent and the methyl group of the oxazoline isopropyl moiety, confirming a proximity that could only be present in the dimeric form. The hydrogen atoms of these moieties are ca. 3.5 Å apart in the X-ray structure of **7**.

Both **7** and **8a** display distorted tetrahedral geometry around the Cu(I) center, where the dihedral angle of (P−Cu−L)−(N−Cu−N) (L = ancillary ligand) differs significantly from 90° [ca. 78.6° (**7**) and 48.6° (**8a**)]. The large distortion of dihedral angle observed for complex **8a** rationalizes the requirement of a bulky ancillary ligand, as **7** is able to achieve a more ideal tetrahedral geometry when **1a** binds $\kappa(P)$, $\kappa^2(NN)$. Particularly diagnostic are the $^{31}P\{^{1}H\}$ NMR shifts for the phosphaalkene resonances in complexes **7** (186 ppm) and **8a** (232 ppm). ^{31}P NMR chemical shifts for phosphaalkene metal complexes have been shown to be sensitive to P−M distance,[31] with shorter P−M bonds having more upfield resonances. Complex **7** possesses a largely upfield $^{31}P\{^{1}H\}$ signal and, accordingly, the P−Cu(I) bond lengths in **7** (ca. 2.17 Å) are shorter than **8a** (ca. 2.31 Å) and other BPEP-Cu(I) complexes [e.g., (BPEP-Ph)Cu(SbF_6), P−Cu: 2.26 and $\delta^{31}P$ = 213;[10] (BPEP-H)Cu(MeCN)$^{+}$, P−Cu: 2.31 Å, and $\delta^{31}P$ = 269[30]].

UV/vis spectroscopic analysis of CH_2Cl_2 solutions of complexes **8a**−**8e** revealed two distinct energy transitions [band I: 450−700 nm and band II: 350−425 nm, Figure 5]. The absorptions in the visible region of the UV spectrum are consistent with the observed colors of **8**: **8a** (λ_{max} = 540 nm,

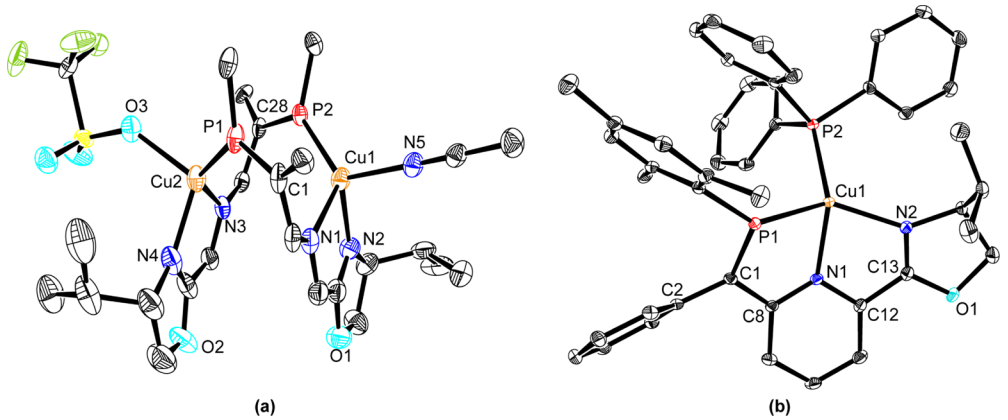

Figure 4. Molecular structures of (a) **7** and (b) **8a**·$(C_4H_8O)_3$. Thermal ellipsoids are drawn at the 50% probability level. (a) Structure truncated to highlight the ligand−metal binding geometry and hydrogens omitted for clarity, (b) hydrogens, THF molecules, and $[OTf]^{-}$ counteranion omitted for clarity. Selected bond lengths (Å) and angles (deg): **7**: P(1)−Cu(2) 2.160(1), P(2)−Cu(1) 2.180(1), N(1)−Cu(1) 2.186(3), N(2)−Cu(1) 2.072(3), N(3)−Cu(2) 2.157(3), N(4)−Cu(2) 2.073(4), P(1)−C(1) 1.694(4), P(2)−C(28) 1.690(3), N(5)−Cu(1) 2.016(3), O(3)−Cu(2) 2.156(8), C(1)−P(1)−Cu(2) 119.8(2), C(28)−P(2)−Cu(1) 121.9(1), N(1)−Cu(1)−P(2) 130.84(8), N(1)−Cu(1)−N(2) 79.6(1), P(2)−Cu(1)−N(2) 115.6(1), P(1)−Cu(2)−N(3) 136.35(8), N(3)−Cu(2)−N(4) 80.2(1), P(1)−Cu(2)−N(4) 118.6(1). **8a**·$(C_4H_8O)_3$: P(1)−C(1) 1.710(2), P(1)−Cu(1) 2.3119(6), P(2)−Cu(1) 2.2263(6), N(1)−Cu(1) 2.043(2), N(2)−Cu(1) 2.072(2), C(1)−C(8) 1.464(3), N(1)−C(8) 1.350(3), N(2)−C(13) 1.281(3), C(12)−C(13) 1.469(3), P(1)−Cu(1)−P(2) 106.10(2), P(1)−Cu(1)−N(1) 78.23(5), P(1)−Cu(1)−N(2) 135.94(5), N(1)−Cu(1)−N(2) 80.34(7), P(2)−Cu(1)−N(2) 115.37(5), N(1)−Cu(1)−P(2) 138.62(6), Cu(1)−P(1)−C(1) 102.70(8), P(1)−C(1)−C(2) 127.2(2), P(1)−C(1)−C(8) 112.4(2), C(12)−C(13)−N(2) 121.9(2), Cu(1)−N(2)−C(13) 110.5(5).

DOI: 10.1021/acs.inorgchem.6b00917
Inorg. Chem. XXXX, XXX, XXX−XXX

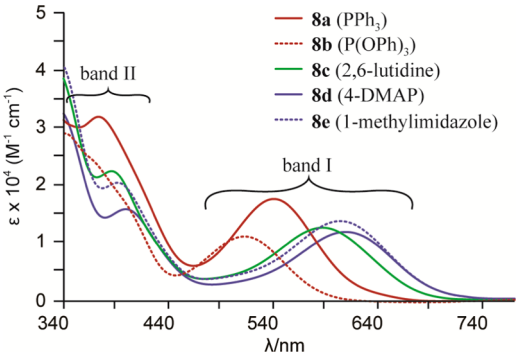

Figure 5. Representative UV/vis spectra of **8a**–**8e** in CH_2Cl_2 solution (all concentrations were ca. 5×10^{-5} mol L^{-1}).

red), **8b** (λ_{max} = 513 nm, red), **8c** (λ_{max} = 587 nm, green), **8d** (λ_{max} = 609 nm, blue), and **8e** (λ_{max} = 604 nm, blue). It is intriguing to note that complexes with the highest energy band I transitions (**8a**, **8b**) also have significantly upfield $^{31}P\{^1H\}$ NMR shifts (Table 1). Conversely, more downfield $^{31}P\{^1H\}$

Table 1. ^{31}P NMR Data (ppm) and λ_{max} Values (nm) for Band I and Band II of 8a–8e

#	L	$\delta^{31}P_{P=C}$	band I: λ_{max} (log ε)	band II: λ_{max} (log ε)
8a	PPh_3	232	540 (4.24)	373 (4.50)
8b	$P(OPh)_3$	227	513 (4.04)	341 (4.46)
8c	2,6-lutidine	215	487 (4.10)	386 (4.35)
8d	4-DMAP	208	609 (4.06)	400 (4.19)
8e	1-methylimidazole	207	604 (4.14)	392 (4.31)

NMR shifts are observed for complexes with low energy band I absorbances (**8d**, **8e**). We hypothesize that an upfield chemical shift is a consequence of a contraction of the =P–Cu(I) bond in complex **8**. Such a bond contraction would be observed for strongly donating ligands (i.e., pyridine and imidazole-based donors) which push electron density toward the Cu(I) center and onto π-accepting phosphaalkene ligand strengthening the =P–Cu(I) interaction. In contrast, where π-accepting ligands [i.e., PPh_3 and $P(OPh)_3$] compete with the π-accepting phosphaalkene ligand, weakening the =P–Cu(I) interaction. This is consistent with that discussed earlier where complex **7**, possessing a shorter =P–Cu bond, was shifted upfield with respect to **8a**. Clearly, these trends are more complex, and additional effects (e.g., sterics) cannot be disregarded. Moreover, more subtle trends in UV/vis and $\delta^{31}P_{P=C}$ have been reported for bis(phosphaalkene) platinum(0) complexes.[32]

Computational Section. To gain further insight into the orbitals involved in the electronic transitions in complex **8** and the trends in λ_{max} (band 1), we modeled **8a** bearing the accepting PPh_3 and **8d** bearing the strongly donating 4-DMAP. Each structure was optimized (Figures S4 and S5, Supporting Information). In the case of **8a**, the optimized structure matched well with that obtained from X-ray crystallography. In the previous section, we hypothesized that the more downfield $^{31}P\{^1H\}$ NMR shift for **8d** is indicative of a shortened P–Cu bond. Accordingly, the computed P–Cu(I) bonds (**8a**: 2.414 Å, **8d**: 2.387 Å) contract when PPh_3 is replaced with 4-DMAP.

Time-dependent DFT (TD-DFT) calculations were performed for **8a** and **8d**, and the frontier molecular orbitals are shown in Figure 6. It is important to note the LUMO is largely composed of the π^*-P=C bond, confirming its π-accepting

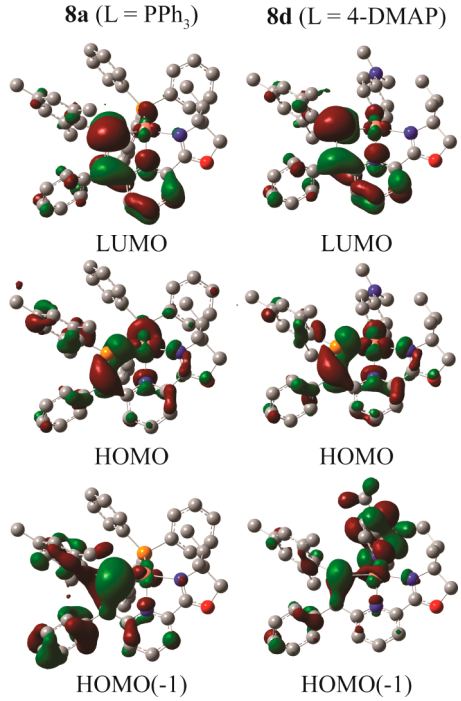

Figure 6. Important molecular orbitals for the low energy transitions of **8a** and **8d**.

ability even vs PPh_3, and its composition does not change significantly with different ancillary ligands. In each complex, the HOMO orbital shows interactions between the pincer ligand and the Cu(I) center. In contrast, the HOMO(−1) are quite different for each complex. In **8a**, the HOMO(−1) is primarily phosphaalkene-based, whereas it consists primarily of DMAP-based electron density in **8d**.

Two absorption bands (I and II) were identified. For **8a**, band I includes major and minor contributions of the HOMO/LUMO (66%), HOMO(−1)/LUMO (15%), HOMO(−3)/LUMO (12%), and HOMO(−4)/LUMO (11%). In contrast, band I of **8d** is composed mainly of the HOMO/LUMO transition (67%). Consistent with the blue shift in band 1 of the UV/vis spectrum, the calculated HOMO–LUMO gap for **8a** (ΔE = 0.297 eV) is larger than for **8d** (ΔE = 0.285 eV). Moreover, the additional mixing of lower energy HOMOs into the band I transition of **8a** may also contribute to the blue shift compared to **8d** which does not show such mixing. For **8a**, band II includes a significant contribution of the HOMO(−1)/LUMO (52%), while band II for **8d** is largely based on the HOMO(−2)/LUMO (64%) transition.

SUMMARY

The synthesis of new tridentate PhAk-Pyr-Ox ligands increases the scope ligand motifs by combining a phosphaalkene and a chiral oxazoline. The spectroscopic properties of Cu(I)-complexes of this new class of pincer ligand highlights the excellent π-accepting properties of these phosphaalkene ligands. In particular, the =P–Cu bond length can be altered by manipulating the electron density around the metal center, which can be observed experimentally by changes in the UV/vis spectra, with different ancillary ligands. A shorter =P–Cu bond length leads to the an upfield $\delta^{31}P_{P=C}$ NMR chemical shift. In addition, red-shifted bands in the UV/vis spectrum suggest a =P–Cu bond contraction. We further investigate

DOI: 10.1021/acs.inorgchem.6b00917
Inorg. Chem. XXXX, XXX, XXX–XXX

this property computationally and propose that, in complexes bearing more electron-rich ancillary ligands (i.e., 4-DMAP), the low-lying $\pi^*_{P=C}$ orbital (the LUMO of these complexes) is able to electronically strengthen the =P−Cu(I) interaction. Future studies will attempt to take advantage of the donor−acceptor properties of these enantiomerically pure pincer ligands in asymmetric catalysis.

EXPERIMENTAL SECTION

Unless stated otherwise, all manipulations were performed using standard Schlenk or glovebox techniques under nitrogen atmosphere. CH_2Cl_2 and hexanes were deoxygenated with nitrogen and dried by passing through a column containing activated alumina. THF was dried over sodium/benzophenone ketyl and distilled prior to use. CD_2Cl_2 and $CDCl_3$ were deoxygenated with nitrogen prior to use. $SOCl_2$, benzene, $AlCl_3$, $(COCl)_2$, Et_3N, NaH, 1-methylimidazole, and $P(OPh)_3$ were purchased from Sigma-Aldrich and used as received. PPh_3 and 4-DMAP were recrystallized from Et_2O prior to use. 2,6-Lutidine was dried over sodium and distilled prior to use. Compounds 6-(methoxycarbonyl)picolinic acid (**4**),[19] $MesP(SiMe_3)_2$,[12] Mes*PH_2,[33] L-valinol,[34] L-phenylanalinol,[34] $Cu(MeCN)_4OTf$[35] were synthesized according to literature procedures. NMR spectra were recorded at 298 K on 300 or 400 MHz spectrometers (operating frequency for ^1H). 85% H_3PO_4 was used as an external standard (δ 0.0) for $^{31}P\{^1H\}$ NMR spectra. $CFCl_3$ in $CDCl_3$ was used as an external solvent (δ 0.0) for $^{19}F\{^1H\}$ NMR spectra. ^1H NMR spectra were referenced to residual protonated solvent, and $^{13}C\{^1H\}$ NMR spectra were referenced to the deuterated solvent. Mass spectra were recorded on a Kratos MS 50 instrument in EI mode (70 eV). Elemental analyses were performed in the UBC Chemistry Microanalysis Facility. The optical rotations were measured at a concentration in g per 100 mL, and their values (average of 10 measurements) were obtained on a Jasco P-1010 polarimeter.

Synthesis of 6-Benzoylpicolinic Acid (2). In air, a suspension of 6-(methoxycarbonyl)picolinic acid (**4**) (30.4 g, 168 mmol) in $SOCl_2$ (79.2 mL, 130 g, 1.09 mol) was heated to reflux for 2 h. The residual $SOCl_2$ was removed by rotary evaporation, the resulting solid was dissolved in benzene (200 mL), and the benzene was removed by rotary evaporation (to remove additional $SOCl_2$). This was repeated two additional times to give the crude acid chloride. A 1-L round-bottom flask was charged with freshly ground $AlCl_3$ (44.8 g, 336 mmol) followed by benzene (250 mL). The suspension was heated to 50 °C, and a solution of the crude acid chloride in benzene (250 mL) was added in one batch with vigorous stirring. The flask was equipped with a reflux condenser and a septum affixed to the condenser with an outlet to an external oil bubbler. The reaction was heated to reflux until the HCl bubbling subsided (ca. 3 h). The reaction was quenched by pouring into a 2-L Erlenmeyer flask containing 100 mL conc. HCl in 500 g of ice. Residual solids in the reaction flask were dissolved in EtOAc and added to the aqueous solution. The organic layer was separated, and the aqueous layer extracted with EtOAc (3 × 200 mL). The organic layers were combined, washed with brine (300 mL), dried over Na_2SO_4, and volatiles were removed by rotary evaporation. The resulting light brown solid was dissolved in 200 mL of CH_2Cl_2 and extracted with 1 M NaOH (3 × 200 mL). The combined aqueous extracts were acidified with 1 M HCl until cloudy and extracted with CH_2Cl_2 (3 × 200 mL). The combined organic layers were dried over Na_2SO_4, and volatiles were removed by rotary evaporation to give the title compound **2** as an off-white solid (26.0 g, 68%).

^1H NMR (400 MHz, $CDCl_3$): δ = 9.08 (br s, 1H), 8.42 (d, J_{HH} = 8 Hz, 1H), 8.27 (d, J_{HH} = 7 Hz, 1H), 8.19 (t, J_{HH} = 8 Hz, 1H), 7.96 (d, J_{HH} = 7 Hz, 1H), 7.64 (t, J_{HH} = 8 Hz, 1H), 7.51 (t, J_{HH} = 7 Hz, 2H); $^{13}C\{^1H\}$ NMR (101 MHz, $CDCl_3$): δ = 192.1, 163.7, 153.5, 144.9, 139.7, 135.3, 133.5, 130.6, 128.5, 128.4, 126.2; HRMS (ESI): m/z 250.0480 (calcd for $NaC_{13}H_{19}NO_3$ 250.0480); Anal. Calcd for $C_{13}H_{19}NO_3$: C, 68.72; H, 3.99; N, 6.16; Found: C, 68.45; H, 4.10; N, 6.15; Mp: 132−134 °C.

Synthesis of (*S*)-PhC=OC_5H_3N(CNOCH(*i*-Pr)−CH_2) (3a). In air, picolinic acid **2** (7.00 g, 30.9 mmol) was suspended in 100 mL of CH_2Cl_2. A few drops of DMF were added, and a septum affixed to the flask with an outlet to an external oil bubbler. $(COCl)_2$ (3.18 mL, 4.71 g, 37.1 mmol) was added dropwise over 30 min, and the reaction was stirred until the bubbling subsided. Volatiles were removed by rotary evaporation to give the crude acid chloride. A 250 mL Schlenk flask was dried and charged with L-valinol (3.43 mL, 3.18 g, 30.9 mmol), Et_3N (21.5 mL, 15.6 g, 150 mmol), and dry CH_2Cl_2 (100 mL). The flask was cooled to 0 °C and a solution of the acid chloride in CH_2Cl_2 (50 mL) was added in one batch. The reaction was warmed to rt and stirred 1 h. The reaction was quenched with sat. $NaHCO_3$ (150 mL), and the organic layer was separated. The organic layer was washed with 1 M HCl (150 mL), separated, and dried over Na_2SO_4. Volatiles were removed by rotary evaporation to give amide **5a** in suitable purity for further reaction.

^1H NMR (400 MHz, $CDCl_3$): δ = 8.28 (dd, J_{HH} = 8, 1 Hz, 1H), 8.12 (dd, J_{HH} = 8, 1 Hz, 1H), 8.05−7.98 (m, 4H), 7.57 (tt, J_{HH} = 8, 1 Hz, 1H), 7.44 (t, J_{HH} = 8 Hz, 2H), 3.90 (m, 1H), 3.72 (dd, J_{HH} = 11, 4 Hz, 1H), 3.65 (dd, J_{HH} = 11, 6 Hz, 1H), 3.40 (br s, 1H), 1.95 (m, 1H), 0.93 (d, J_{HH} = 7 Hz, 3H), 0.86 (d, J_{HH} = 7 Hz, 3H).

In a 500 mL round-bottom flask, the amide **5a** synthesized in the previous step was dissolved in 200 mL of $CHCl_3$. $SOCl_2$ (13.4 mL, 22.1 g, 185 mmol) was added and the flask was equipped with a reflux condenser. The reaction was heated to reflux for 3 h and cooled to rt, and the volatiles removed by rotary evaporation. The residual oil was dissolved in EtOAc (50 mL) filtered through a silica plug (ca. 8″) using EtOAc as the eluent. The EtOAc was removed by rotary evaporation to give chloride **6a** in suitable purity for further reaction.

^1H NMR (400 MHz, $CDCl_3$): δ = 8.35 (dd, J_{HH} = 8, 1 Hz, 1H), 8.20 (dd, J_{HH} = 8, 1 Hz, 1H), 8.08−7.98 (m, 4H), 7.57 (tt, J_{HH} = 8, 2 Hz, 1H), 7.45 (t, J_{HH} = 8 Hz, 2H), 4.10 (m, 1H), 3.72 (dd, J_{HH} = 11, 4 Hz, 1H), 3.67 (dd, J_{HH} = 11, 4 Hz, 1H), 1.97 (m, 1H), 0.96 (d, J_{HH} = 7 Hz, 3H), 0.89 (d, J_{HH} = 7 Hz, 3H).

A 250 mL Schlenk flask was dried and charged with chloride **6a** synthesized in the previous step and NaH (60% dispersion in oil, 1.80 g, 46.4 mmol) (*Note: for reactions involving greater than 100 mmol, dry 95% NaH should be used as an excess of oil can impede purification). The solids were suspended in dry THF (125 mL) and heated to reflux for 3 h. The reaction was cooled to rt, and the sodium salts were removed by filtration (*Note: do not use Celite or silica as a filter medium, as accidental hydrolysis can take place). The volatiles were removed by rotary evaporation, and the resulting oil was triturated with pentane to give a brown/red solid. The solid was collected by filtration and recrystallized in Et_2O to give the title compound **3a** as a light yellow solid (4.12 g, 45% over three steps). Single crystals suitable for X-ray diffraction analysis were obtained after a concentrated solution of **3a** in Et_2O was left in a−30 °C freezer.

^1H NMR (400 MHz, $CDCl_3$): δ = 8.20 (d, J_{HH} = 8 Hz, 1H), 8.13 (d, J_{HH} = 7 Hz, 2H), 7.99 (d, J_{HH} = 8 Hz, 1H), 7.88 (t, J_{HH} = 8, 1H), 7.49 (t, J_{HH} = 7, 1H), 7.39 (t, J_{HH} = 8, 2H), 4.43 (m, 1H), 4.11 (m, 2H), 1.80 (m, 1H), 0.98 (d, J_{HH} = 7 Hz, 3H), 0.88 (d, J_{HH} = 7 Hz, 3H); $^{13}C\{^1H\}$ NMR (101 MHz, $CDCl_3$): δ = 192.1, 161.9, 154.7, 145.7, 137.3, 135.4, 132.9, 131.1, 127.9, 126.0, 125.8, 72.6, 70.7, 32.6, 18.7, 18.1; HRMS (ESI): m/z 317.1260 (calcd for $C_{18}H_{18}N_2O_2Na$ 317.1266); Anal. Calcd for $C_{18}H_{18}N_2O_2$: C, 73.45; H, 6.16; N, 9.52; Found: C, 73.30; H, 6.21; N, 9.38; $[\alpha]_D^{22}$ = −118° cm^3 g^{-1} dm^{-1} (c = 2.2 × 10^{-1}, $CHCl_3$).

Synthesis of Synthesis of (*S*)-PhC=OC_5H_3N(CNOCH-(CH_2Ph)−CH_2) (3b). Ketone **3b** was synthesized in an analogous fashion to **3a**: picolinic acid **2** (5.60 g, 24.8 mmol), $COCl_2$ (3.77 g, 29.7 mmol), L-phenylalaninol (3.75 g, 24.8 mmol), and Et_3N (12.5 g, 124 mmol) to make the corresponding pyridyl amide **5b**. ^1H NMR (400 MHz, $CDCl_3$): δ = 8.23 (dd, J_{HH} = 8, 1 Hz, 1H), 8.15 (d, J_{HH} = 9 Hz, 1H), 8.02 (dd, J_{HH} = 8, 1 Hz, 1H), 7.98−7.88 (m, 3H), 7.56 (tt, J_{HH} = 8, 2 Hz, 1H), 7.43 (t, J_{HH} = 8 Hz, 2H), 7.17−7.07 (m, 5H), 4.35 (m, 1H), 3.82−3.62 (m, 2H), 3.03−2.81 (m, 3H).

$SOCl_2$ (17.7 g, 150 mmol) in $CHCl_3$ (125 mL) was used to produce the crude chloride **6b**.

^1H NMR (400 MHz, $CDCl_3$): δ = 8.38 (dd, J_{HH} = 8, 1 Hz, 1H), 8.24 (dd, J_{HH} = 8, 1 Hz, 1H), 8.19−8.06 (m, 4H), 7.67 (tt, J_{HH} = 7, 2 Hz, 1H), 7.54 (t, J_{HH} = 8 Hz, 2H), 7.25−7.19 (m, 5H), 4.62 (m, 1H),

DOI: 10.1021/acs.inorgchem.6b00917
Inorg. Chem. XXXX, XXX, XXX−XXX

3.70 (dd, J_{HH} = 11, 4 Hz, 1H), 3.60 (dd, J_{HH} = 11, 3 Hz, 1H), 3.00 (m, 2H).

NaH (0.893 g, 37.2 mmol) in THF (100 mL) was used to produce the crude product, which was recrystallized in Et_2O to give the title compound **3b** as an off-white solid (5.64 g, 66% over three steps).

^{1}H NMR (400 MHz, $CDCl_3$): δ = 8.26 (d, J_{HH} = 8 Hz, 1H), 8.20 (d, J_{HH} = 8 Hz, 2H), 8.07 (d, J_{HH} = 8 Hz, 1H), 7.95 (t, J_{HH} = 8 Hz, 1H), 7.57 (d, J_{HH} = 7 Hz, 1H), 7.47 (t, J_{HH} = 8 Hz, 2H), 7.32−7.21 (m, 5H), 4.65 (m, 1H), 4.44 (t, J_{HH} = 9 Hz, 1H), 4.22 (t, J_{HH} = 8 Hz, 1H), 3.24 (dd, J_{HH} = 14, 5 Hz, 1H), 2.80 (dd, J_{HH} = 14, 9 Hz, 1H); ^{13}C{^{1}H} NMR (101 MHz, $CDCl_3$): δ = 192.2, 162.6, 154.9, 145.6, 137.5, 137.5, 133.0, 131.2, 129.1, 128.4, 128.0, 126.4, 126.1, 126.0, 72.4, 67.9, 41.4; HRMS (ESI): m/z 343.1447 (calcd for $C_{22}H_{19}N_2O_2$ 343.1451); Anal. Calcd for $C_{22}H_{18}N_2O_2$: C, 77.17; H, 5.30; N, 8.18; Found: C, 77.10; H, 5.35; N, 8.17; $[\alpha]_D^{22}$ = −47.6° cm^3 g^{-1} dm^{-1} (c = 2.8 × 10^{-1}, $CHCl_3$).

Synthesis of (*S*)-MesP═CPhC$_5$H$_3$N(CNOCH(*i*-Pr)−CH$_2$) (1a). To a solution of MesP(SiMe$_3$)$_2$ (1.85 g, 6.24 mmol) in THF (10 mL) was added methyllithium (1.6 M, 3.9 mL, 6.24 mmol). The reaction mixture was heated to 55 °C for 1−2 h. ^{31}P NMR analysis of an aliquot removed from the reaction mixture suggested quantitative formation of MesP(Li)SiMe$_3$ (δ = −187). The reaction mixture was cooled to −78 °C and treated with a solution of ketone **3a** (1.67 g, 5.67 mmol) in THF (5 mL). After being warmed to room temperature, analysis of an aliquot removed from the reaction mixture by ^{31}P NMR spectroscopy revealed two singlet resonances consistent with phosphaalkene (*E*/*Z*-**1a**) (δ = 248/267 ppm). The reaction mixture was quenched with excess SiMe$_3$Cl (ca. 3 mL), and the solvent was evaporated in vacuo. The product was extracted into toluene (10 mL and 2 × 5 mL) and filtered. The toluene was evaporated in vacuo, and the resultant red paste precipitated with hexanes (10 mL). The solid was filtered and dried in vacuo to give the product as a pink solid (1.3 g, 54%). Single crystals of *Z*-**1a** suitable for X-ray diffraction analysis were obtained by slow evaporation of a C_6H_6 solution of *E*/*Z*-**1a**.

^{31}P{^{1}H} NMR (162 MHz, $CDCl_3$): δ = 248.3 (*Z*), 266.6 (*E*); ^{1}H NMR (400 MHz, $CDCl_3$, *Z*-isomer): δ = 7.75 (d, J_{HH} = 8 Hz, 1H), 7.60−7.56 (m, 2H), 7.44 (t, J_{HH} = 8 Hz, 1H), 7.35−7.26 (m, 3H), 6.94 (d, J_{HH} = 8 Hz, 1H), 6.61 (s, 2H), 4.45−4.39 (m, 1H), 4.19−4.07 (m, 2H), 2.32 (s, 6H), 2.13 (s, 3H), 1.90−1.83 (m, 1H), 1.04 (d, J_{HH} = 7 Hz, 3H), 0.94 (d, J_{HH} = 7 Hz, 3H); ^{1}H NMR (400 MHz, $CDCl_3$, *E*-isomer): δ = 8.10 (d, J_{HH} = 8 Hz, 1H), 7.62 (t, J_{HH} = 8 Hz, 1H), 7.14 (d, J_{HH} = 8 Hz, 1H), 7.12−7.06 (m, 3H), 6.92−6.88 (m, 2H), 6.68 (s, 2H), 4.62−4.55 (m, 1H), 4.30−4.22 (m, 1H), 4.14−4.07 (m, 1H), 2.26 (s, 3H), 2.25 (s, 3H), 2.18 (s, 3H), 1.93−1.86 (m, 1H), 1.10 (d, J_{HH} = 7 Hz, 3H), 0.98 (d, J_{HH} = 7 Hz, 3H); ^{13}C NMR data only provided for the major *Z*-isomer:^{13}C{^{1}H} NMR (101 MHz, $CDCl_3$): δ = 191.5 (d, J_{PC} = 41 Hz), 162.7, 160.7, 160.1, 146.0, 142.3 (d, J_{PC} = 23 Hz), 140.4 (br s), 138.0, 136.7, 135.6, 128.9 (d, J_{PC} = 5 Hz), 128.2, 127.5, 126.5 (d, J_{PC} = 22 Hz), 124.7 (d, J_{PC} = 6 Hz), 123.2, 121.8, 72.5, 70.4, 32.6, 22.4 (d, J_{PC} = 8 Hz), 20.9, 18.8, 18.0; MS (EI): m/z [%] 430, 429, 428 [3, 29, 100, M$^+$], 386, 385 [4, 17, M$^+$-CHMe$_2$]; HRMS (EI): m/z 428.2016 (calcd for $C_{27}H_{29}N_2OP$ 428.2018).

Synthesis of (*S*)-Mes*P═CPhC$_5$H$_3$N(CNOCH(*i*-Pr)−CH$_2$) (1b). To a cooled (−78 °C) solution of MesPH$_2$ (1.35 g, 4.85 mmol) in THF (15 mL) was added *n*-butyllithium (1.6 M in hexanes, 3.6 mL, 5.81 mmol). The reaction was warmed to room temperature and stirred 1 h. The solution was cooled (−78 °C), and TMSCl (0.63 g, 5.81 mmol) was added. The reaction was warmed to room temperature and immediately cooled (−78 °C), and *n*-butyllithium (1.6 M in hexanes, 3.3 mL, 5.34 mmol) was added. The reaction was stirred 1 h and ketone **6a** (1.14 g, 3.88 mmol) in THF (5 mL) was added to the cooled solution, and the mixture was allowed to warm to room temperature. The reaction was quenched with excess TMS-Cl (ca. 1 mL), and the solvent was evaporated *in vacuo*. At this point the product could be handled under ambient moisture and air. The product was dissolved in hexanes (ca. 3 mL) and filtered through a small plug of Celite. Volatiles were removed using rotary evaporation, and the yellow residue was purified by column chromatography (neutral Al_2O_3, 1:10 EtOAc:hexanes as the eluent) to give *E*/*Z*-**1b** as a yellow solid (0.59 g, 27%).

^{31}P{^{1}H} NMR (121 MHz, $CDCl_3$): δ = 266.0 (*E*), 257.6 (*Z*); ^{1}H and ^{13}C NMR assigned only for major Z-isomer: ^{1}H NMR (400 MHz, $CDCl_3$): δ = 7.71 (d, J_{HH} = 8 Hz, 1H), 7.56−7.53 (m, 2H), 7.37−7.33 (m, 3H), 7.24−7.20 (m, 3H), 6.49 (d, J_{HH} = 8 Hz, 1H), 4.49−4.42 (m, 1H), 4.18−4.06 (m, 2H), 1.90−1.86 (m, 1H), 1.57 (s, 9H), 1.55 (s, 9H), 1.32 (s, 9H), 1.09 (d, J_{HH} = 7 Hz, 3H), 0.97 (d, J_{HH} = 7 Hz, 3H); ^{13}C{^{1}H} NMR (101 MHz, $CDCl_3$): δ = 179.0 (d, J_{PC} = 45 Hz), 163.0, 159.2 (d, J_{PC} = 14 Hz), 154.6 (d, J_{PC} = 41 Hz), 149.9, 145.8, 143.9, 143.6, 136.2, 134.7, 134.3, 129.1 (d, J_{PC} = 8 Hz), 128.1, 127.8, 127.6, 125.9 (d, J_{PC} = 6 Hz), 121.9, 121.3, 121.2, 72.5, 70.5, 38.1, 34.8 (d, J_{PC} = 15 Hz), 33.5, 33.5, 33.3 (d, J_{PC} = 6 Hz), 32.8, 31.3; MS (ESI): m/z 579, 578 [35, 100, M-Na$^+$]; HRMS (ESI): m/z 555.3491 (calcd for $C_{36}H_{48}N_2OP$ 555.3504).

Synthesis of (*S*)-MesP═CPhC$_5$H$_3$N(CNOCH(CH$_2$Ph)−CH$_2$) (1c). **1c** was synthesized in an analogous fashion to **1a**: MesP(SiMe$_3$)$_2$ (1.05 g, 3.53 mmol), and ketone **6b** (1.10 g, 3.21 mmol) in THF (10 mL) was used to produce the crude product, which was extracted with toluene and washed with Et_2O to give the title compound *E*/*Z*-**1c** as a pink solid (0.64 g, 42%).

^{31}P{^{1}H} NMR (121 MHz, $CDCl_3$): δ = 264.4 (Z), 245.5 (E); ^{1}H NMR assigned only for major E-isomer: ^{1}H NMR (400 MHz, $CDCl_3$): δ = 8.07 (d, J_{HH} = 8 Hz, 1H), 7.65 (t, J_{HH} = 8 Hz, 1H), 7.36−7.22 (m, 5H), 7.16 (d, J_{HH} = 8 Hz, 1H), 7.12−7.08 (m, 3H), 6.91−6.87 (m, 2H), 6.68 (s, 2H), 4.69−4.65 (m, 1H), 4.50 (t, J_{HH} = 9 Hz, 1H), 4.29 (t, J_{HH} = 8 Hz, 1H), 3.31 (dd, J_{HH} = 13, 5 Hz, 1H), 2.79 (dd, J_{HH} = 14, 9 Hz, 1H), 2.25 (s, 6H), 2.19 (s, 3H); MS (EI): m/z 477, 476 [37, 100, M$^+$], 386, 385 [20, 76, M$^+$-CH$_2$Ph], 240, 239 [15, 74, MesPCPh$^+$], 92, 91 [6, 45, PhCH$_2^+$]; HRMS (EI): m/z 476.2018 (calcd for $C_{31}H_{29}N_2OP$ 476.2018).

Synthesis of [Cu$_2$(1a)$_2$(OTf)(MeCN)]OTf (7). A solution of phosphaalkene **1a** (0.40 g, 0.932 mmol) and Cu(MeCN)$_4$OTf (0.36 g, 0.932 mmol) in CH_2Cl_2 (10 mL) was stirred for 2 h. The solution was concentrated to 5 mL in vacuo, and the product was precipitated with Et_2O (ca. 10 mL). The suspension was stirred 30 min and filtered, and dried in vacuo to give **7** as a brown solid (0.49 g, 79%). Single crystals suitable for X-ray diffraction analysis were obtained by slow diffusion of Et_2O into a CH_2Cl_2 solution of **7**.

^{31}P{^{1}H} NMR (162 MHz, $CDCl_3$): δ = 186.0; ^{1}H NMR (400 MHz, $CDCl_3$): δ = 8.04 (m, 4H), 7.43 (d, J_{HH} = 8 Hz, 2H), 7.22 (br s, 2H), 7.1 (br s, 8H), 6.85 (s, 2H), 6.06 (s, 2H), 4.48 (t, J_{HH} = 10 Hz, 2H), 4.37 (t, J_{HH} = 9 Hz, 2H), 2.75 (s, 6H), 2.32 (m, 2H), 2.17 (s, 6H), 2.04 (s, 3H), 1.83 (m, 2H), 1.29 (s, 6H), 1.02 (d, J_{HH} = 6 Hz, 6H), 0.83 (d, J_{HH} = 7 Hz, 6H); ^{13}C{^{1}H} NMR (101 MHz, $CDCl_3$): δ = 117.4 (m), 166.7, 160.4, 143.5, 142.6, 141.7, 140.7, 139.9, 130.6, 130.0, 129.9, 129.5, 129.4, 129.1, 128.7, 125.0, 74.0, 70.7, 32.3, 23.5, 21.7, 21.5, 18.9, 17.6, 2.6; ^{19}F{^{1}H} NMR (114 MHz, $CDCl_3$): δ = −78.2; Anal. Calcd for $C_{58}H_{61}Cu_2F_6N_5O_8P_2S_2$: C, 52.64; H, 4.65; N, 5.29; Found: C, 52.44; H, 4.74; N, 4.93; $[\alpha]_D^{22}$ = −24.7°cm^3 g^{-1} dm^{-1} (c = 1.8 × 10^{-1}, CH_2Cl_2).

Synthesis of [Cu(1a)(PPh$_3$)]OTf (8a). A solution of complex **7** (100 mg, 0.075 mmol) and PPh$_3$ (40 mg, 0.150 mmol) in CH_2Cl_2 (3 mL) was stirred for 30 min. The solution was concentrated and the resultant red residue was triturated with hexanes (2 mL). The solid was filtered and washed with additional hexanes (2 × 2 mL) and dried in vacuo to give **8a** as a red solid (90 mg, 67%). Single crystals suitable for X-ray diffraction analysis were obtained by slow diffusion of hexanes into a THF solution of **8a**.

^{31}P{^{1}H} NMR (162 MHz, CD_2Cl_2): δ = 231.7, 8.9; ^{1}H NMR (400 MHz, CD_2Cl_2): δ = 8.12 (d, J_{HH} = 8 Hz, 1H), 8.01 (t, J_{HH} = 8 Hz, 1H). 7.79 (d, J_{HH} = 8 Hz, 1H), 7.43−7.21 (m, 21 H), 7.10 (br s, 2H), 6.91 (s, 1H), 6.16 (s, 1H), 4.60 (m, 1H), 4.50 (m, 1H), 2.99 (m, 1H), 2.65 (s, 3H), 2.19 (s, 3H), 1.62 (m, 1H), 1.01 (s, 3H), 0.83 (d, J_{HH} = 7 Hz, 3H), 0.72 (d, J_{HH} = 7 Hz, 3H); ^{13}C{^{1}H} NMR (101 MHz, CD_2Cl_2): δ = 171.8, 167.0, 156.4 (d, J_{PC} = 9 Hz), 144.1 (d, J_{PC} = 20 Hz), 142.2, 140.9, 139.1, 138.6, 138.0 (d, J_{PC} = 12 Hz), 133.7 (d, J_{PC} = 14 Hz), 131.3, 130.8 (d, J_{PC} = 25 Hz), 129.5, 129.4, 129.3, 129.0, 125.6 (d, J_{PC} = 9 Hz), 123.5, 75.6, 69.9, 33.1, 23.2 (d, J_{PC} = 22 Hz), 22.2, 21.2, 18.5, 18.3; ^{19}F{^{1}H} NMR (114 MHz, $CDCl_3$): δ = −78.6;

DOI: 10.1021/acs.inorgchem.6b00917
Inorg. Chem. XXXX, XXX, XXX−XXX

HRMS (EI): m/z 640.0839 (calcd for $C_{28}H_{29}O_4N_2PF_3{}^{63}CuS$ 640.0834); $[\alpha]_D^{22}$ = 89.2° $cm^3\ g^{-1}\ dm^{-1}$ ($c = 0.72 \times 10^{-1}$, CH_2Cl_2).

Representative Addition of a Neutral Ligand to Complex 7 (8b–e). A solution of complex **7** (3 mg, 5 μmol) and L (5 μmol) in CH_2Cl_2 (0.7 mL) was sonicated for 30 min. The brown color of complex **7** immediately changed to either a deep red (L = $P(OPh)_3$), deep green (L = 2,6-lutidine), or deep blue (L = 4-DMAP or 1-methylimidazole) color. Subsequent $^{31}P\{^1H\}$ NMR analysis of the mixture revealed quantitative conversion to a new product.

$^{31}P\{^1H\}$ NMR (162 MHz, CH_2Cl_2): δ = 227.2, 114.3 (L = $P(OPh)_3$), 214.7 (L = 2,6-lutidine), 208.4 (L = 4-DMAP), 207.4 (L = 1-methylimidazole).

X-ray Crystallography. All single crystals were immersed in oil and mounted on a glass fiber. Data were collected on a Bruker X8 APEX II diffractometer with graphite-monochromated Mo Kα radiation. All structures were solved by direct methods and subsequent Fourier difference techniques. All non-hydrogen atoms were refined anisotropically with hydrogen atoms being included in calculated positions but not refined. All data sets were corrected for absorption effects (SADABS), Lorentz, and polarization effects. All calculations were performed using SHELXL-2014 crystallographic software package from Bruker AXS.[36] Absolute configuration was confirmed on the basis of the refined Flack parameter.[37] Compound **7** crystallizes with positional disorder for the chelating $-OSO_2CF_3$ ligand. Their respective populations were refined to the final occupancy of 0.564(4) {S(1), O(3), O(4), O(5), C(57), F(1a), F(2a), F(3a)} and 0.436(4) {S(1a), O(3a), O(4a), O(5a), C(57a), F(1), F(2), F(3)}. Compound **8a** recrystallizes with two ordered molecules of THF and a disordered molecule of THF in the asymmetric unit, but only one atom could be located on using the difference map and was refined anisotropically. Their respective populations were refined to the final occupancy of 0.77(1) {C(52)} and 0.23(1) {C(52a)}. Additional crystal data and details of data collection and structure refinement are listed in Table S5 in the Supporting Information. All crystallographic data has been deposited with the Cambridge Structural Database: 1469495, 1469496, 1469497, 1469498.

Computational Details. All calculations were performed with Gaussian 09[38] using the B3LYP density function.[39−42] The full compounds were first optimized using the minimal basis set 6-31G(d,p)[43,44] using an initial geometry obtained from a solid state molecular structure when available. Final optimization and TD-B3LYP calculations were preformed using the superior TZVP basis set.[45]

■ ASSOCIATED CONTENT

Supporting Information

The Supporting Information is available free of charge on the ACS Publications website at DOI: 10.1021/acs.inorgchem.6b00917.

Additional NMR spectra, optimized structures of **8a** and **8d**, and crystallographic details (PDF)

Crystallographic data for **3a** (CIF)

Crystallographic data for *Z*-**1a** (CIF)

Crystallographic data for **7** (CIF)

Crystallographic data for **8a** (CIF)

Cartesian coordinates for the calculated structures **8a** (XYZ) and **8d** (XYZ)

■ AUTHOR INFORMATION

Corresponding Authors

*(G.R.D.) E-mail: gdake@chem.ubc.ca.

*(D.P.G.) E-mail: dgates@chem.ubc.ca.

Notes

The authors declare no competing financial interest.

■ ACKNOWLEDGMENTS

The authors thank the Natural Sciences and Engineering Research Council (NSERC) of Canada for financial support in the form of Discovery, Strategic, and Research Tools & Instruments grants to G.D. and D.G.

■ REFERENCES

(1) (a) van Koten, G. J. *J. Organomet. Chem.* **2013**, *730*, 156−164. (b) Schneider, S.; Meiners, J.; Askevold, B. *Eur. J. Inorg. Chem.* **2012**, *2012*, 412−429. (c) Benito-Garagorri, D.; Kirchner, K. *Acc. Chem. Res.* **2008**, *41*, 201−213. (d) Nishiyama, H. *Chem. Soc. Rev.* **2007**, *36*, 1133−1141. (e) *Organometallic Pincer Chemistry*; van Koten, G., Milstein, D., Eds.; Springer-Verlag: Berlin, 2003. (f) Albrecht, M.; van Koten, G. *Angew. Chem., Int. Ed.* **2001**, *40*, 3750−3781.

(2) For examples and applications of nonsymmetric PNN pincer ligands, see: (**A**) (a) Cheisson, T.; Auffrant, A. *Dalton Trans.* **2016**, *45*, 2069−2078. (b) Butschke, B.; Fillman, K. L.; Bendikov, T.; Shimon, L. J. W.; Diskin-Posner, Y.; Leitus, G.; Gorelsky, S. I.; Neidig, M. L.; Milstein, D. *Inorg. Chem.* **2015**, *54*, 4909−4926. (c) Feller, M.; Diskin-Posner, Y.; Shimon, L. J. W.; Ben-Ari, E.; Milstein, D. *Organometallics* **2012**, *31*, 4083−4101. (d) Balaraman, E.; Ben-David, Y.; Milstein, D. *Angew. Chem., Int. Ed.* **2011**, *50*, 11702−11705. (e) Balaraman, E.; Fogler, E.; Milstein, D. *Chem. Commun.* **2012**, *48*, 1111−1113. (f) Balaraman, E.; Gnanaprakasam, B.; Shimon, L. J. W.; Milstein, D. *J. Am. Chem. Soc.* **2010**, *132*, 16756−16758. (g) Zhang, J.; Leitus, G.; Ben-David, Y.; Milstein, D. *J. Am. Chem. Soc.* **2005**, *127*, 10840−10841. (**B**) (h) Chen, T.; Li, H.; Qu, S.; Zheng, B.; He, L.; Lai, Z.; Wang, Z.-X.; Huang, K.-W. *Organometallics* **2014**, *33*, 4152−4155. (i) He, L.-P.; Chen, T.; Gong, D.; Lai, Z.; Huang, K.-W. *Organometallics* **2012**, *31*, 5208−5211. (j) Zeng, G.; Chen, T.; He, L.; Pinnau, I.; Lai, Z.; Huang, K.-W. *Chem. - Eur. J.* **2012**, *18*, 15940−15943. (k) Chen, T.; He, L.-P.; Gong, D.; Yang, L.; Miao, X.; Eppinger, J.; Huang, K.-W. *Tetrahedron Lett.* **2012**, *53*, 4409−4412.

(3) For selected reviews highlighting P═C bonds in coordination chemistry, see (a) Müller, C.; Broeckx, L. E. E.; de Krom, I.; Weemers, J. J. M. *Eur. J. Inorg. Chem.* **2013**, *2013*, 187−202. (b) Dugal-Tessier, J.; Conrad, E.; Dake, G. R.; Gates, D. P. In *Phosphorus(III) Ligands in Homogenous Catalysis: Design and Synthesis*; Kamer, P. C. J., van Leeuwen, P. W. N. M., Eds.; Wiley: Chichester, 2012; Chapter 10. (c) Müller, C.; Vogt, D. *Dalton Trans.* **2007**, 5505−5523. (d) Le Floch, P. *Coord. Chem. Rev.* **2006**, *250*, 627−681. (e) Ozawa, F.; Yoshifuji, M. *Dalton Trans.* **2006**, 4987−4995. (f) Weber, L. *Angew. Chem., Int. Ed.* **2002**, *41*, 563−572.

(4) For recent work highlighting P═C bonds in coordination chemistry, see (a) Chang, Y.; Tanigawa, I.; Taguchi, H.; Takeuchi, K.; Ozawa, F. *Eur. J. Inorg. Chem.* **2016**, *2016*, 754−760. (b) Klein, M.; Schnakenburg, G.; Espinosa Ferao, A.; Streubel, R. *Dalton Trans.* **2016**, *45*, 2085−2094. (c) Rigo, M.; Sklorz, J. A. W.; Hatje, N.; Noack, F.; Weber, M.; Wiecko, J.; Muller, C. *Dalton Trans.* **2016**, *45*, 2218−2226. (d) Magnuson, K. W.; Oshiro, S. M.; Gurr, J. R.; Yoshida, W. Y.; Gembicky, M.; Rheingold, A. L.; Hughes, R. P.; Cain, M. F. *Organometallics* **2016**, *35*, 855−859. (e) Masuda, J. D.; Boere, R. T. *Dalton Trans.* **2016**, *45*, 2102−2115. (f) Ghalib, M.; Jones, P. G.; Schulzke, C.; Sziebert, D.; Nyulászi, L.; Heinicke, J. W. *Inorg. Chem.* **2015**, *54*, 2117−2127. (g) Ueta, Y.; Mikami, K.; Ito, S. *Inorg. Chem.* **2015**, *54*, 8778−8785. (h) Greenacre, V. K.; Trathen, N.; Crossley, I. R. *Organometallics* **2015**, *34*, 2533−2542. (i) Takeuchi, K.; Minami, A.; Nakajima, Y.; Ozawa, F. *Organometallics* **2014**, *33*, 5365−5370. (j) Broeckx, L. E. E.; Lutz, M.; Vogt, D.; Müller, C. *Chem. Commun.* **2011**, *47*, 2003−2005.

(5) Doux, M.; Moores, A.; Mézailles, N.; Ricard, L.; Jean, Y.; Floch, P. L. *J. Organomet. Chem.* **2005**, *690*, 2407−2415.

(6) Additional pyridine-based low-valent phosphorus pincer ligand motifs are reported in (a) Müller, C.; Pidko, E. A.; Lutz, M.; Spek, A. L.; Vogt, D. *Chem. - Eur. J.* **2008**, *14*, 8803−8807. (b) Ekici, D. G.; Nieger, M.; Nyulaszi, L.; Niecke, E.; Gudat, D. *Angew. Chem., Int. Ed.* **2002**, *41*, 3367−3371.

DOI: 10.1021/acs.inorgchem.6b00917
Inorg. Chem. XXXX, XXX, XXX−XXX

(7) Jouaiti, A.; Geoffroy, M.; Bernardinelli, G. *Tetrahedron Lett.* **1992**, *33*, 5071−5074.
(8) Nakajima, Y.; Nakao, Y.; Sakaki, S.; Tamada, Y.; Ono, T.; Ozawa, F. *J. Am. Chem. Soc.* **2010**, *132*, 9934−9936.
(9) Lin, Y.-F.; Ichihara, N.; Nakajima, Y.; Ozawa, F. *Organometallics* **2014**, *33*, 6700−6703.
(10) Nakajima, Y.; Shiraishi, Y.; Tsuchimoto, T.; Ozawa, F. *Chem. Commun.* **2011**, *47*, 6332−6334.
(11) Nakajima, Y.; Tsuchimoto, T.; Chang, Y.-H.; Takeuchi, K.; Ozawa, F. *Dalton Trans.* **2016**, *45*, 2079−2084.
(12) Yam, M.; Chong, J. H.; Tsang, C.-W.; Patrick, B. O.; Lam, A. E.; Gates, D. P. *Inorg. Chem.* **2006**, *45*, 5225−5234.
(13) Dugal-Tessier, J.; Dake, G. R.; Gates, D. P. *Organometallics* **2007**, *26*, 6481−6486.
(14) Dugal-Tessier, J.; Dake, G. R.; Gates, D. P. *Angew. Chem., Int. Ed.* **2008**, *47*, 8064−8067.
(15) Dugal-Tessier, J.; Serin, S. C.; Castillo-Contreras, E. B.; Conrad, E. D.; Dake, G. R.; Gates, D. P. *Chem. - Eur. J.* **2012**, *18*, 6349−6359.
(16) Dugal-Tessier, J.; Dake, G. R.; Gates, D. P. *Org. Lett.* **2010**, *12*, 4667−4669.
(17) Daugulis, O.; Brookhart, M.; White, P. S. *Organometallics* **2002**, *21*, 5935−5943.
(18) (a) Desimoni, G.; Faita, G.; Quadrelli, P. *Chem. Rev.* **2003**, *103*, 3119−3154. (b) Evans, D. A.; Fandrick, K. R.; Song, H.; Scheidt, K. A.; Xu, R. *J. Am. Chem. Soc.* **2007**, *129*, 10029−10041. (c) Wei, C.; Li, C. *J. Am. Chem. Soc.* **2002**, *124*, 5638−5639. (d) Evans, D. A.; Kozlowski, M. C.; Murry, J. A.; Burgey, C. S.; Campos, K. R.; Connell, B. T.; Staples, R. J. *J. Am. Chem. Soc.* **1999**, *121*, 669−685. (e) Evans, D. A.; Barnes, D. M.; Johnson, J. S.; Lectka, R.; von Matt, P.; Miller, S. J.; Murry, J. A.; Norcross, R. D.; Shaughnessy, E. A.; Campos, K. R. *J. Am. Chem. Soc.* **1999**, *121*, 7582−7594. (f) Nishiyama, H.; Kondo, M.; Nakamura, T.; Itoh, K. *Organometallics* **1991**, *10*, 500−508.
(19) Ong, W. Q.; Zhao, H.; Du, Z.; Yeh, J. Z. Y.; Ren, C.; Tan, L. Z. W.; Zhang, K.; Zeng, H. *Chem. Commun.* **2011**, *47*, 6416−6418.
(20) Ito, F.; Ando, S.; Iuchi, M.; Ukari, T.; Takasaki, M.; Yamaguchi, K. *Tetrahedron* **2011**, *67*, 8009−8013.
(21) Desimoni, G.; Faita, G.; Quadrelli, P. *Chem. Rev.* **2003**, *103*, 3119−3154.
(22) Rawe, B. W.; Chun, C. P.; Gates, D. P. *Chem. Sci.* **2014**, *5*, 4928−4938.
(23) Lipshutz, B. H.; Shimizu, H. *Angew. Chem., Int. Ed.* **2004**, *43*, 2228−2230.
(24) Lipshutz, B. H.; Noson, K.; Chrisman, W. *J. Am. Chem. Soc.* **2001**, *123*, 12917−12918.
(25) Li, Z.; Quan, R. W.; Jacobsen, E. N. *J. Am. Chem. Soc.* **1995**, *117*, 5889−5890.
(26) Wei, C.; Li, C.-J. *J. Am. Chem. Soc.* **2002**, *124*, 5638−5639.
(27) Degrado, S. J.; Mizutani, H.; Hoveyda, A. H. *J. Am. Chem. Soc.* **2001**, *123*, 755−756.
(28) d'Augustin, M.; Palais, L.; Alexakis, A. *Angew. Chem., Int. Ed.* **2005**, *44*, 1376−1378.
(29) Orthaber, A.; Belaj, F.; Pietschnig, R. *Inorg. Chim. Acta* **2011**, *374*, 211−215.
(30) Hayashi, A.; Okazaki, M.; Ozawa, F.; Tanaka, R. *Organometallics* **2007**, *26*, 5246−5249.
(31) Nakajima, Y.; Nakatani, M.; Hayashi, K.; Shiraishi, Y.; Takita, R.; Okazaki, M.; Ozawa, F. *New J. Chem.* **2010**, *34*, 1713−1722.
(32) Hayashi, K.; Nakatani, M.; Hayashi, A.; Takano, M.; Okazaki, M.; Toyota, K.; Yoshifuji, M.; Ozawa, F. *Organometallics* **2008**, *27*, 1970−1972.
(33) Bresien, J.; Faust, K.; Schulz, A.; Villinger, A. *Angew. Chem., Int. Ed.* **2015**, *54*, 6926−6930.
(34) McKennon, M. J.; Meyers, A. I.; Drauz, K.; Schwarm, M. *J. Org. Chem.* **1993**, *58*, 3568−3571.
(35) Irangu, J. K.; Jordan, R. B. *Inorg. Chem.* **2003**, *42*, 3934−3942.
(36) Sheldrick, G. M. *Acta Crystallogr., Sect. A: Found. Crystallogr.* **2008**, *64*, 112−122.
(37) Parsons, S.; Flack, H. D.; Wagner, T. *Acta Crystallogr., Sect. B: Struct. Sci., Cryst. Eng. Mater.* **2013**, *69*, 249−259.
(38) Frisch, M. J.; Trucks, G. W.; Schlegel, H. B.; Scuseria, G. E.; Robb, M. A.; Cheeseman, J. R.; Scalmani, G.; Barone, V.; Mennucci, B.; Petersson, G. A.; Nakatsuji, H.; Caricato, M.; Li, X.; Hratchian, H. P.; Izmaylov, A. F.; Bloino, J.; Zheng, G.; Sonnenberg, J. L.; Hada, M.; Ehara, M.; Toyota, K.; Fukuda, R.; Hasegawa, J.; Ishida, M.; Nakajima, T.; Honda, Y.; Kitao, O.; Nakai, H.; Vreven, T.; Montgomery, J. A., Jr., Peralta, J. E.; Ogliaro, F.; Bearpark, M. J.; Heyd, J.; Brothers, E. N.; Kudin, K. N.; Staroverov, V. N.; Kobayashi, R.; Normand, J.; Raghavachari, K.; Rendell, A. P.; Burant, J. C.; Iyengar, S. S.; Tomasi, J.; Cossi, M.; Rega, N.; Millam, N. J.; Klene, M.; Knox, J. E.; Cross, J. B.; Bakken, V.; Adamo, C.; Jaramillo, J.; Gomperts, R.; Stratmann, R. E.; Yazyev, O.; Austin, A. J.; Cammi, R.; Pomelli, C.; Ochterski, J. W.; Martin, R. L.; Morokuma, K.; Zakrzewski, V. G.; Voth, G. A.; Salvador, P.; Dannenberg, J. J.; Dapprich, S.; Daniels, A. D.; Farkas, Ö.; Foresman, J. B.; Ortiz, J. V.; Cioslowski, J.; Fox, D. J. *GAUSSIAN 09*; Gaussian, Inc.: Wallingford, CT, USA, 2009.
(39) Stephens, P. J.; Devlin, F. J.; Chabalowski, C. F.; Frisch, M. J. *J. Phys. Chem.* **1994**, *98*, 11623−11627.
(40) Becke, A. D. *J. Chem. Phys.* **1993**, *98*, 5648−5652.
(41) Lee, C.; Yang, W.; Parr, R. G. *Phys. Rev. B: Condens. Matter Mater. Phys.* **1988**, *37*, 785−789.
(42) Vosko, S. H.; Wilk, L.; Nusair, M. *Can. J. Phys.* **1980**, *58*, 1200−1211.
(43) Francl, M. M.; Pietro, W. J.; Hehre, W. J.; Binkley, J. S.; Gordon, M. S.; DeFrees, D. J.; Pople, J. A. *J. Chem. Phys.* **1982**, *77*, 3654−3665.
(44) Dill, J. D.; Pople, J. A. *J. Chem. Phys.* **1975**, *62*, 2921−2923.
(45) Schäfer, A.; Huber, C.; Ahlrichs, R. *J. Chem. Phys.* **1994**, *100*, 5829−5835.

DOI: 10.1021/acs.inorgchem.6b00917
Inorg. Chem. XXXX, XXX, XXX−XXX